NASA TECHNICAL NOTE

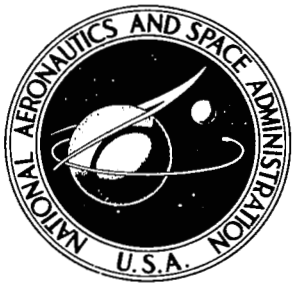

NASA TN D-6640

NASA TN D-6640

REYNOLDS NUMBER EFFECT ON OVERALL PERFORMANCE OF A 10.8-CENTIMETER (4.25-IN.) SWEPTBACK-BLADED CENTRIFUGAL COMPRESSOR

by Carl Weigel and Calvin L. Ball

Lewis Research Center
Cleveland, Ohio 44135

NATIONAL AERONAUTICS AND SPACE ADMINISTRATION • WASHINGTON, D. C. • JANUARY 1972

1. Report No.	2. Government Accession No.	3. Recipient's Catalog No.
NASA TN D-6640		

4. Title and Subtitle	5. Report Date
REYNOLDS NUMBER EFFECT ON OVERALL PERFORMANCE OF A 10.8-CENTIMETER (4.25-IN.) SWEPTBACK-BLADED CENTRIFUGAL COMPRESSOR	January 1972
	6. Performing Organization Code

7. Author(s)	8. Performing Organization Report No.
Carl Weigel and Calvin L. Ball	E-6586
	10. Work Unit No. 764-74

9. Performing Organization Name and Address	11. Contract or Grant No.
Lewis Research Center National Aeronautics and Space Administration Cleveland, Ohio 44135	
	13. Type of Report and Period Covered
12. Sponsoring Agency Name and Address	Technical Note
National Aeronautics and Space Administration Washington, D.C. 20546	14. Sponsoring Agency Code

15. Supplementary Notes

16. Abstract

Experimental overall performance is given for a range of compressor Reynolds numbers from 0.34×10^6 to 3.03×10^6. The performance data were taken at 50 000 rpm, using argon gas. As the Reynolds number was reduced from near design value to 30 percent of design, the maximum efficiency decreased about 1.5 percentage points. Reducing the Reynolds number from 30 percent to approximately 10 percent of design caused the maximum efficiency to decrease another 2.5 percentage points. The variation in loss with Reynolds number is compared with the commonly used inverse power relation of loss with Reynolds number.

17. Key Words (Suggested by Author(s))	18. Distribution Statement
Centrifugal compressor Turbomachinery Space power Brayton cycle	Unclassified - unlimited

19. Security Classif. (of this report)	20. Security Classif. (of this page)	21. No. of Pages	22. Price*
Unclassified	Unclassified	22	$3.00

* For sale by the National Technical Information Service, Springfield, Virginia 22151

REYNOLDS NUMBER EFFECT ON OVERALL PERFORMANCE OF A 10.8-CENTIMETER (4.25-IN.) SWEPTBACK-BLADED CENTRIFUGAL COMPRESSOR

by Carl Weigel and Calvin L. Ball

Lewis Research Center

SUMMARY

Experimental overall performance for a 10.8-centimeter (4.25-in.) centrifugal compressor with sweptback blades is given for a range of compressor Reynolds numbers. The compressor was designed for a Brayton cycle space power system with a nominal design output of 6 kilowatts, with a range of 2 to 10 kilowatts. For this investigation, the compressor was operated at a speed of 50 000 rpm, with an inlet temperature of 300 K (540° R) using argon gas. Overall performance was obtained for seven inlet pressure levels, from 13.7 to 1.6 N/cm^2 abs (19.9 to 2.3 psia). This range of inlet pressures resulted in a Reynolds number range based on tip diameter of 3.03×10^6 to 0.34×10^6. As Reynolds number was decreased, the maximum efficiency point and surge point moved progressively to lower flow rates. The maximum flow rate also decreased as Reynolds number decreased. The maximum efficiency decreased about 1.5 percentage points (0.813 to 0.800) as the Reynolds number was reduced from near design (3.03×10^6) to about 30 percent of design (0.88×10^6). Further reduction of the Reynolds number to about 10 percent of design (0.34×10^6) caused the maximum efficiency to decrease 2.5 percentage points more (0.800 to 0.775). By using the inverse power relation of loss with Reynolds number that is commonly used as an approximate correlation, a power of $n = 0.1$ was found to closely approximate the slope of the loss Reynolds number curve.

INTRODUCTION

The Lewis Research Center is conducting investigations on the closed Brayton cycle system for space vehicle onboard electrical power generation (refs. 1 and 2). In support of the Brayton cycle studies, experimental investigations are being conducted to

determine the effect that Reynolds number has on the performance of small centrifugal- and axial-flow compressors applicable to these systems (refs. 3 to 5). The turbomachinery for space power systems generally operates at lower Reynolds numbers than the turbomachinery designed for airbreathing engine applications. This is due to the smaller size machines being considered for space power systems, along with lower cycle pressure ratios. The lower cycle pressure ratios result in lower required blade speeds and lower associated relative flow velocities in the compressor and turbine. Adequate theoretical or empirical correlations are not available for small compressors to accurately predict the loss in performance that results from a low design Reynolds number or the subsequent change in performance as Reynolds number is changed. The difficulty in arriving at such a loss correlation is due to the complexity of the flow in the compression process and the subdivision of the associated losses. Of the total compressor loss, which has many origins, only that portion associated with viscous fluid effects has been directly related to Reynolds number. We recognize, however, the potential influence of boundary layer growth or viscous effects on the other loss components, such as those losses associated with secondary flows. At present, no method is available to accurately calculate the magnitude of the viscous loss. The percent of the total loss resulting from viscous effects is, in part, dependent on the particular compressor design, such as the type of inducer, the impeller design, the type of diffuser, and the aerodynamic match between the various components. An assessment of the use of conventional aerodynamic parameters, the mechanisms causing losses, and the problem of geometric dissimilarities of turbomachinery in predicting the effect of Reynolds number and efficiency is given in references such as references 6 to 8.

To minimize development time and cost of the turbomachinery for a Brayton cycle space power system, it is desirable to be able to take a basic set of hardware that is designed for a nominal power level and be able to use it for a range of power outputs. This can be accomplished by adjusting the system pressure level. When the system pressure level is changed, the Reynolds number at which the turbomachinery must operate is changed. Since sufficient experimental data for small compressors are not available to accurately predict the change in compressor performance (both efficiency and weight flow) with changes in Reynolds number, an experimental program is being conducted at the Lewis Research Center to better establish the Reynolds number influence on compressor performance. This is in support of Brayton cycle system studies such as those given in references 9 and 10.

This report gives the performance of a 10.8-centimeter (4.25-in.) sweptback-bladed centrifugal compressor for a range of Reynolds numbers. The overall performance of this compressor at design inlet conditions was reported in reference 11. The compressor was designed for a single-shaft Brayton cycle system having a nominal design electrical power output of 6 kilowatts, with a range of 2 to 10 kilowatts. The AiResearch Mfg. Co. of Phoenix, Arizona, designed and fabricated the compressor (ref. 12). The

compressor Reynolds number in this investigation was varied from 0.34×10^6 to 3.03×10^6 by varying the inlet pressure from 1.6 to 13.7 N/cm^2 abs (2.3 to 19.9 psia). The inlet temperature was set at the design value of 300 K (540° R) for all tests. The compressor was operated at a speed of 50 000 rpm, using argon gas as the working fluid. The performance results given in this report were obtained from tests conducted at the Lewis Research Center.

COMPRESSOR DESIGN

The compressor was designed for a nominal 6-kilowatt, single-shaft, Brayton cycle space electrical power system. The working fluid specified for the system was a mixture of helium-xenon (HeXe) gas having a molecular weight of 83.8. Argon gas was used for this test program instead of the design gas mixture of helium-xenon because it had the same specific-heat ratio and was more readily available. The compressor design is presented in reference 12. A summary of the compressor design-point values for argon gas and equivalent values based on standard inlet pressure and temperature are given in table I for the reference design power level.

TABLE I. - COMPRESSOR DESIGN PARAMETERS FOR ARGON GAS

Inlet total pressure, P_1, N/cm^2 abs; psia	13.96; 20.25
Inlet total temperature, T_1, K; $^\circ$R	300; 540
Weight flow rate, w, kg/sec; lbm/sec	0.356; 0.785
Equivalent weight flow, $w\sqrt{\theta}/\delta$, kg/sec; lbm/sec	0.263; 0.581
Overall total-pressure ratio, P_6/P_1	1.9
Overall total-temperature ratio, T_6/T_1	1.37
Overall efficiency, η_{1-6}	0.80
Impeller total-pressure ratio, P_3/P_1	2.03
Impeller efficiency, η_{1-3}	0.895
Rotative speed, RPM, rpm	52 200
Equivalent speed, RPM/$\sqrt{\theta}$, rpm	51 176
Impeller tip speed, U_{t3}, m/sec; ft/sec	295; 968
Equivalent impeller tip speed, $U_{t3}/\sqrt{\theta}$, m/sec; ft/sec	289; 949
Compressor work factor, f_{cw}	0.658
Specific speed, N_s	0.11
Reynolds number, Re_U	3.1×10^6

The compressor impeller has 15 blades that are curved backward at the exit 30° from the radial direction. The impeller inlet blade tip diameter is 6.60 centimeters (2.60 in.) and the hub diameter is 3.66 centimeters (1.44 in.). The impeller exit tip diameter is 10.8 centimeters (4.25 in.) and the exit blade height is 0.521 centimeter

(0.205 in.). Design velocity diagrams for the impeller inlet and outlet are shown in figure 1 for argon gas.

From the impeller exit to the vaned diffuser inlet, there is a vaneless diffuser section about 0.216 centimeter (0.085 in.) long in the radial direction. The vaned diffuser section has 17 vanes of constant height (0.541 cm, or 0.213 in.). The diffuser design velocity diagrams for argon gas are shown in figure 2.

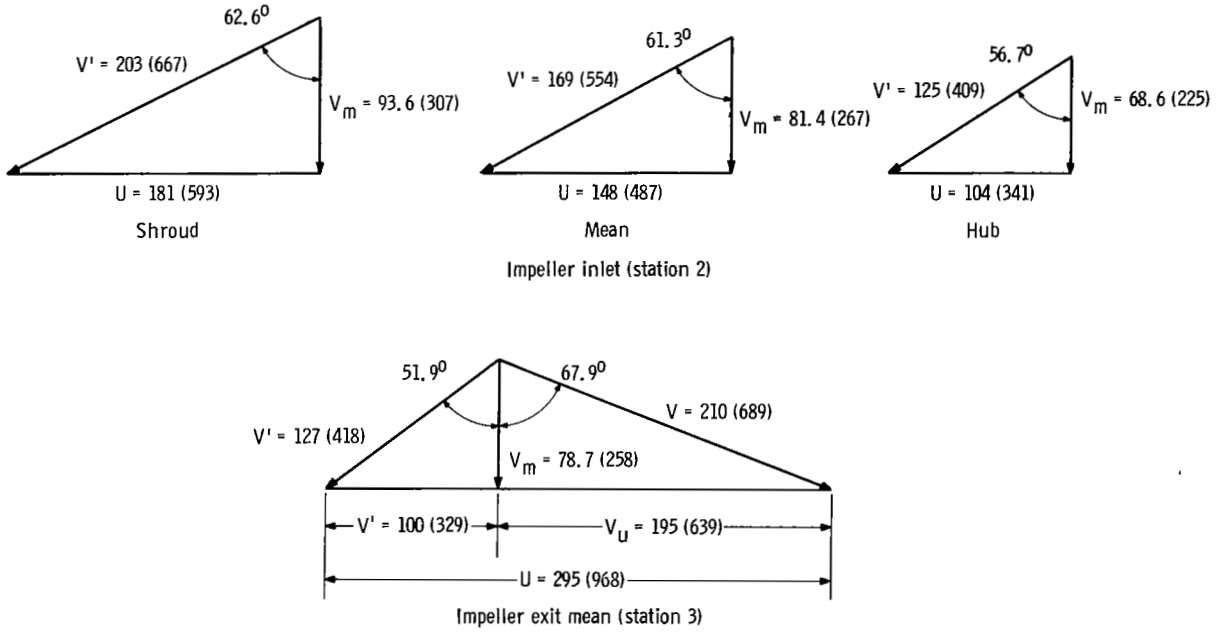

Figure 1. - Impeller design velocity diagrams for argon gas. All velocities in meters per second (ft/sec).

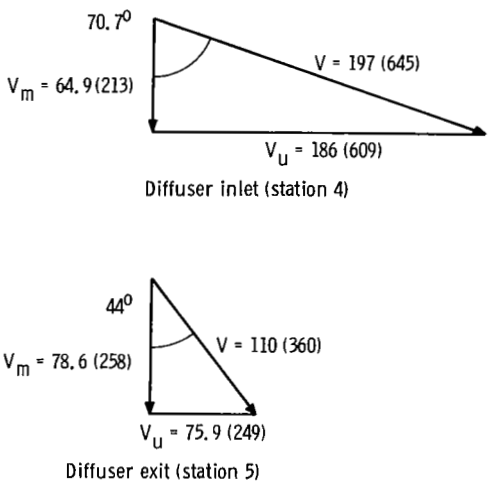

Figure 2. - Diffuser design velocity diagrams for argon gas. All velocities in meters per second (ft/sec).

APPARATUS AND PROCEDURE

Test Apparatus

The impeller and vaned diffuser used in this investigation are shown in figure 3. The impeller was cantilever-mounted on a shaft supported by two spring-loaded angular contact bearings. An air-oil mist system was used to lubricate and cool the bearings. A

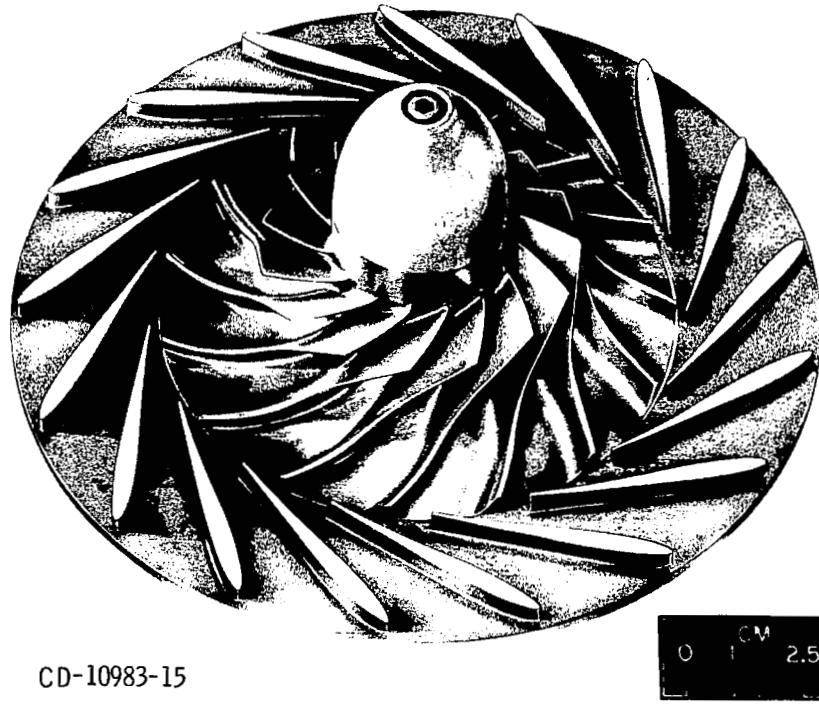

CD-10983-15

Figure 3. - Compressor impeller and vaned diffuser. Impeller exit diameter, 10. 8 centimeters (4. 25 in.).

carbon face seal was located outboard of the bearing on the impeller end of the shaft, and a labyrinth seal was used on the other end. The static (cold) impeller clearance between the shroud and the impeller exit blade tip was set at 0.020 centimeter (0.008 in.). The compressor was fully enclosed in insulation. A cutaway view of the compressor with locations of instrument and calculation stations is shown in figure 4. More details of the compressor test facility and apparatus are given in reference 11.

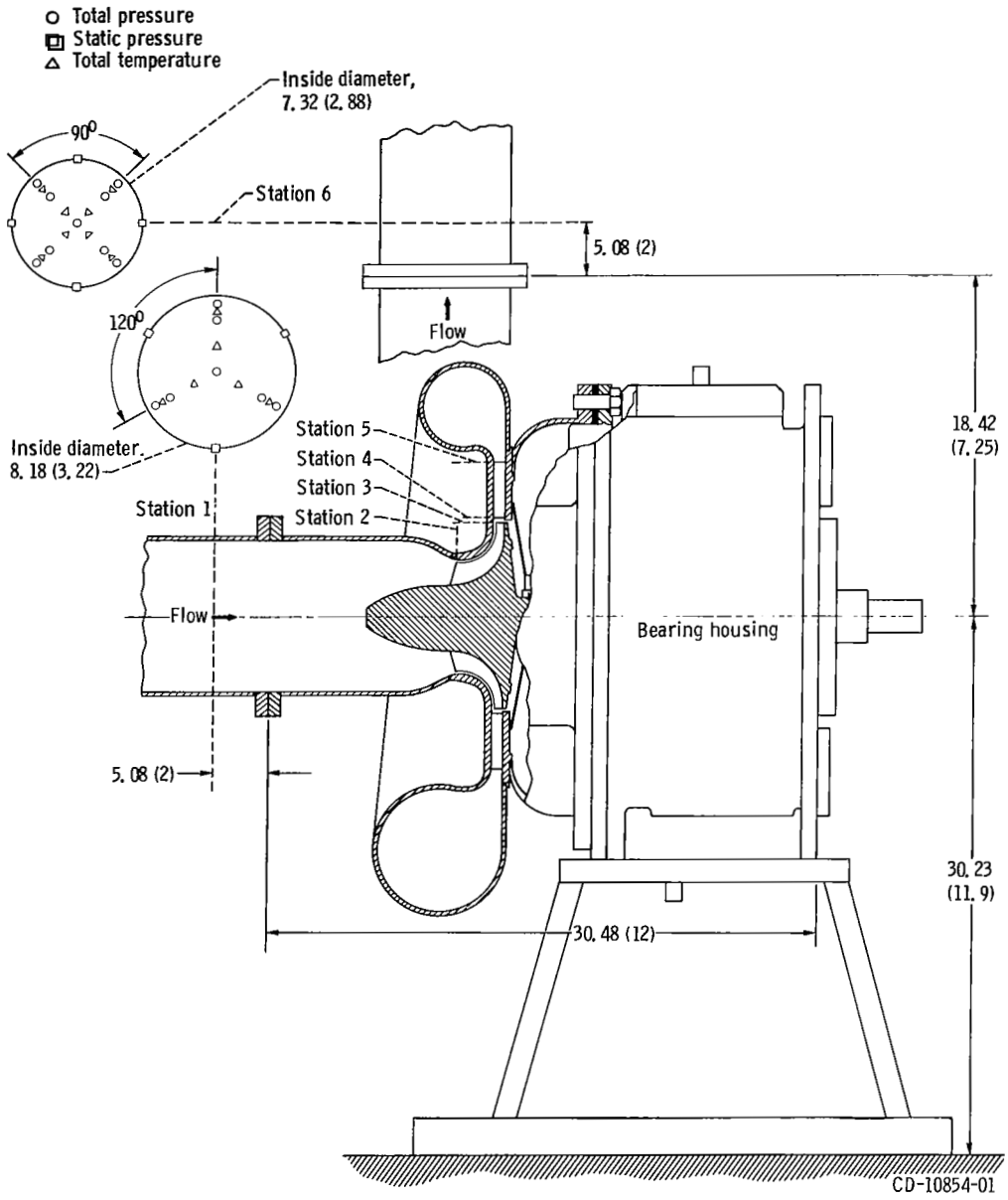

Figure 4. - Compressor cross section, showing instrument locations at stations 1 and 6. All dimensions are in centimeters (in.).

Test Procedure

Compressor performance was taken at a speed of 50 000 rpm for seven different inlet pressures, from 1.6 to 13.7 N/cm^2 abs (2.3 to 19.9 psia). For each inlet pressure the flow was varied from near maximum to compressor surge. The inlet temperature

was set at 300 K (540° R) and was essentially constant for all tests. The tests were run at 50 000 rpm because a severe shaft vibration occurred at the design speed of 52 200 rpm (for argon gas).

During operation, a significant change in the character of compressor surge takes place. At the higher inlet pressures ($P_1 > 10.1$ N/cm^2 abs (6 psia)) the compressor surge was abrupt, with violent pressure oscillations. At the very low inlet pressures the surge or stall pressure oscillations were very mild and almost undetectable due to the low density of the gas. Because of this, the minimum flow point at the very low inlet pressures was obtained at a flow rate just above the point where a rapid increase in inlet temperature, due to recirculation, was detected.

Calculation Procedure

The total-pressure ratio, temperature rise ratio, and adiabatic efficiency were computed from measured pressures and temperatures obtained at stations 1 and 6 (fig. 4). The performance parameters are given in appendix A. The compressor Reynolds number Re_U was computed by using the inlet total density ρ_1, impeller exit tip speed U_{t3}, impeller exit tip diameter D_{t3}, and inlet dynamic viscosity μ_1. The overall efficiency presented herein was calculated using the exit temperature that was obtained from the inner ring of thermocouples (station 6, fig. 4). For all pressure levels below the design inlet pressure it was apparent that the outer ring of thermocouples was being appreciably affected by heat transfer. At the lower inlet pressures even the inner ring did not appear to provide for an accurate indication of the temperature rise across the compressor. Therefore, for the lower pressures an extrapolation of the temperatures measured by the inner ring of thermocouples at the higher inlet pressures was used. A comparison between the temperatures measured by the inner and outer rings of thermocouples is given in appendix B. Included is the extrapolation made to obtain the exit temperature at the very low inlet pressures.

RESULTS AND DISCUSSION

The following results were obtained from a 10.8-centimeter (4.25-in.) sweptback-bladed centrifugal compressor using argon gas as the working fluid. All performance was taken at 50 000 rpm, 96 percent of design equivalent speed, with an inlet temperature of 300 K (540° R).

The overall total-pressure ratio as a function of percent of design equivalent weight flow is shown in figure 5 for seven different inlet pressures. The corresponding com-

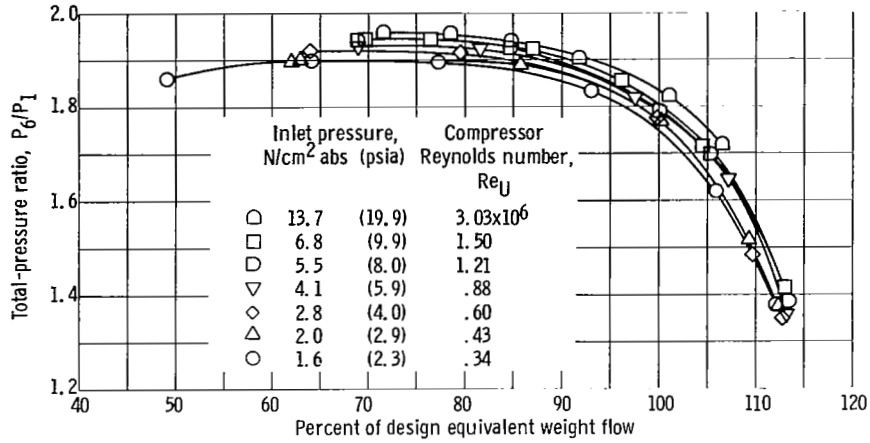

Figure 5. - Total-pressure ratio as function of percent of design equivalent weight flow, for seven inlet pressures, at 96 percent of design equivalent speed.

pressor Reynolds number based on tip diameter is shown for each inlet pressure. The peak total-pressure ratio progressively decreased from 1.96 to 1.90 as the inlet pressure was reduced from 13.7 N/cm^2 abs (19.9 psia) to 1.6 N/cm^2 abs (2.3 psia). This change in inlet pressure corresponds to a change in compressor Reynolds number of 3.03×10^6 to 0.34×10^6. The compressor maximum flow rate generally decreased with decreasing inlet pressure. The flow rate at which compressor surge occurred also decreased with decreasing inlet pressure. This trend can be partially attributed to increasing boundary layer thickness with decreasing Reynolds number. The increased boundary layer thickness in the compressor reduces the effective flow areas, which in turn causes an increase in through-flow velocity of the gas. This resulting increase in the through-flow (radial) velocity at the impeller exit decreases the absolute tangential velocity or whirl of the fluid. This in turn reduces the absolute flow angle leaving the impeller and changes the incidence angle of the flow entering the vaned diffuser. This incidence angle strongly influences the flow range over which the compressor may operate and the point at which maximum efficiency occurs. The flow rate at which the maximum efficiency and surge occur can therefore be expected to vary with Reynolds number. The maximum flow rate should also behave in a like manner.

The ratio of compressor total-temperature rise to inlet total temperature as a function of percent of design equivalent weight flow is shown in figure 6. Because of heat-transfer effects, the exit temperatures were based on the inner ring of thermocouples, with the temperature obtained at the higher inlet pressures being extrapolated to obtain the temperatures used for the lower inlet pressures (see appendix B). The resulting temperature rise ratio is essentially constant with inlet pressure.

The adiabatic efficiency for each different pressure level is shown in figure 7 as a function of percent of design equivalent weight flow. The highest efficiency occurred at

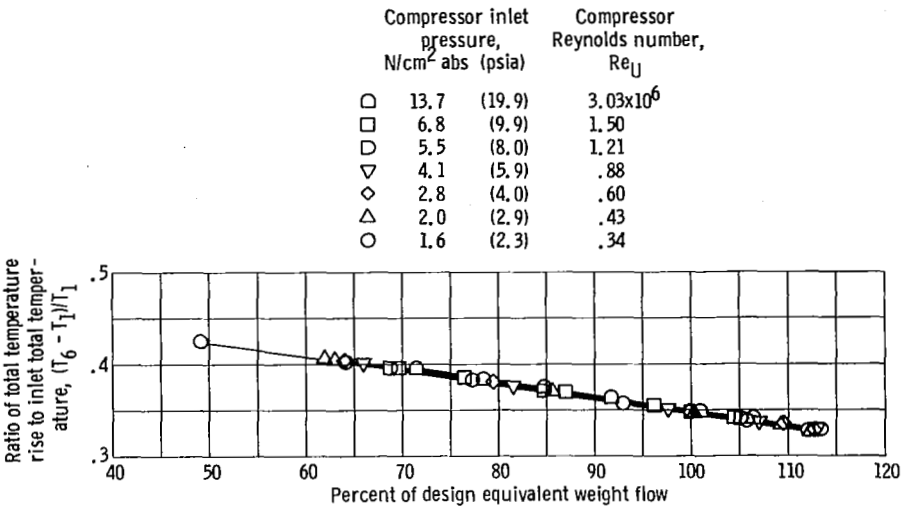

Figure 6. - Ratio of compressor total-temperature rise to inlet temperature as function of percent of design equivalent weight flow, for seven inlet pressures, at 96 percent of design equivalent speed.

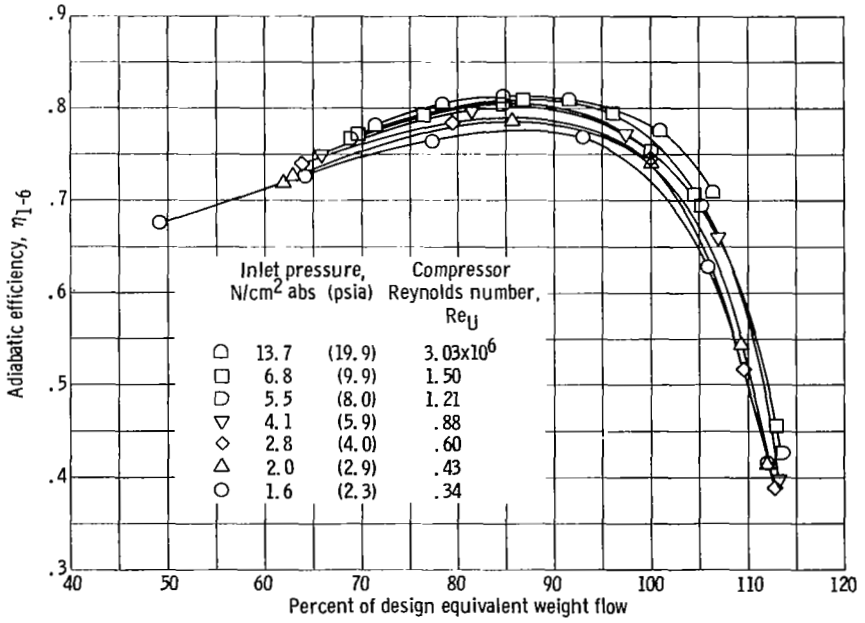

Figure 7. - Overall adiabatic efficiency as function of percent of design equivalent weight flow, for seven inlet pressures, at 96 percent of design equivalent speed.

about 87.5 percent of design equivalent weight flow at design inlet pressure. The maximum efficiency point decreased with each decrease in inlet pressure. The maximum efficiency point also moved to a slightly lower flow rate with each decrease in inlet pressure. Although the maximum efficiency was obtained at a flow rate less than design, unpublished data using this rotor indicate that by changing the diffuser vane setting angle, the maximum efficiency can be moved to a higher flow rate. The influence of the diffuser vane setting angle on controlling compressor flow range and the weight flow at which peak efficiency occurs is also shown in reference 13 for a 15.2-centimeter (6-in.) radial-bladed centrifugal compressor. The gain in performance of the 6-kilowatt Brayton cycle power system when the maximum efficiency point is moved to a higher flow rate is indicated in reference 10.

The maximum efficiency points of figure 7 are shown as a function of design Reynolds number in figure 8. This figure shows a drop in maximum compressor efficiency of

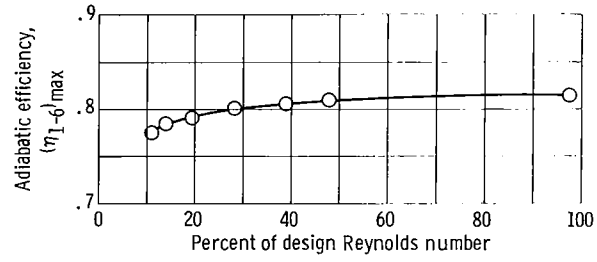

Figure 8. - Maximum adiabatic efficiency as function of percent of design Reynolds number at 96 percent of design equivalent speed. Design $Re_U = 3.1 \times 10^6$.

about 1.5 percentage points as Reynolds number or inlet pressure is reduced to about 30 percent of the design value. (This compared to operating the system at 2-kW output for the 6-kW system.) Operation below 30 percent of design Reynolds number resulted in a more rapid decrease in maximum efficiency. The maximum efficiency dropped about 2.5 percentage points as the Reynolds number was reduced from 30 percent to 10 percent of design.

One relationship that has been used in an attempt to correlate loss with Reynolds number for compressors is

$$\frac{1 - \eta}{1 - \eta_{ref}} = \left[\frac{(Re_U)_{ref}}{Re_U}\right]^n$$

where η_{ref} and $(Re_U)_{ref}$ are known values of efficiency and Reynolds number (ref. 14). The exponent n has been found to have an approximately constant value in the range of

0.1 to 0.25 (ref. 15). The loss $1 - \eta_{max}$ as a function of compressor Reynolds number is shown in figure 9. A dashed line for $n = 0.2$, which is commonly used for this range of Reynolds numbers, is shown for comparison with the loss curve. For the dashed $n = 0.2$ line, a Reynolds number of 3.03×10^6 (near design) and the corresponding loss of 0.187 were chosen as the reference conditions. The rate that the losses increase with

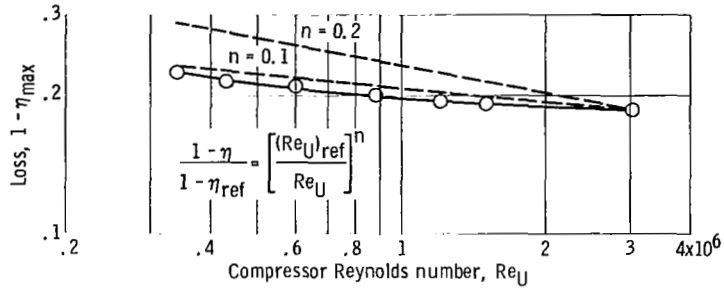

Figure 9. - Loss as function of compressor Reynolds number at 96 percent of design equivalent speed. Design $Re_U = 3.1 \times 10^6$.

decreasing Reynolds number is less than that predicted by $n = 0.2$. A value of $n = 0.1$ more closely approximates the loss curve. For a closer approximation of the loss with Reynolds number than is given by a single value of $n = 0.1$, the data can be roughly divided into three parts and the following experimental values of n applied for the corresponding Reynolds number range:

$$n = 0.06, \quad 1.21 \times 10^6 < Re_U < 3.03 \times 10^6$$

$$n = 0.09, \quad 0.43 \times 10^6 < Re_U < 1.21 \times 10^6$$

$$n = 0.2, \quad 0.34 \times 10^6 < Re_U < 0.43 \times 10^6$$

The trend in the data obtained from this compressor illustrates the point stated in reference 6, that the Reynolds number influence does not necessarily follow the simple power law but appears to follow a variable exponential function where the exponent is a function of Reynolds number, increasing with decreasing Reynolds number. As the Reynolds number becomes increasingly large (greater than 1×10^6, fig. 9) the loss approaches a constant value, and the exponent n approaches zero (ref. 16). This is the same trend that the boundary layer thickness has been shown to exhibit on a flat plate (ref. 7) and in pipes and ducts (ref. 17). As turbulent flow is fully developed at the higher Reynolds numbers the laminar sublayer at the wall diminishes, and surface roughness precludes further reduction of the losses. The wall is described as aerodynamically rough when the rough-

ness elements protrude through the laminar sublayer, and increasing Reynolds number has little or no effect on the losses. (The surface finish of the internal flow passages of this compressor was approximately 81.3×10^{-6} cm (32 μin.) rms.) From the trend shown by the loss Reynolds number curve of figure 9 it would appear that the flow passages were aerodynamically smooth for the major portion of this test.

The overall compressor Reynolds number Re_U, as defined, has been primarily useful in predicting performance changes in machines having geometric similarity, using the same fluid under dynamically similar conditions. The loss Reynolds number performance obtained from the two geometrically similar radial-bladed centrifugal compressors reported in references 3 and 4 showed close agreement, as would be expected. However, the higher efficiency achieved by this centrifugal compressor over the same Reynolds number range can be attributed to design differences. The impeller designs are different (sweptback blades/radial blades), and the vaned diffusers are different (two-dimensional-vane island-type blading/three-dimensional airfoil-type vanes).

In conclusion, the results of this investigation, when compared with the results of references 3 and 4, illustrate some of the inadequacies (which have been known for some time, for example, ref. 8) of the commonly used centrifugal compressor Reynolds number. As defined, the same Reynolds number can be obtained for compressors that are geometrically dissimilar with different specific speeds. And the same fluid velocity distribution or flow regime in different parts of the machine cannot be assured. These problems, of course, are secondary to the difficulty encountered in obtaining accurate experimental data when the pressure is lowered to obtain low Reynolds numbers. Temperatures and pressures become difficult to measure. When the energy addition to the gas is determined by the temperature rise, heat transfer in or out of the system becomes a significant problem, with the rate of heat transfer being a function of Reynolds number. As stated in reference 7, it is not surprising that attempts at general correlations of compressor Reynolds number data show a great deal of scatter. The decrease in maximum efficiency that resulted from decreasing the compressor inlet pressure illustrates the significance of the Reynolds number influence on the compressor performance for the intended application.

SUMMARY OF RESULTS

A 10.8-centimeter (4.25-in.) centrifugal compressor with sweptback blades was run at 50 000 rpm, 96 percent of design speed, with an inlet temperature of 300 K (540° R) using argon gas. Overall performance was obtained for seven different inlet pressures, from 13.7 to 1.6 N/cm^2 abs (19.9 to 2.3 psia). This gave a change in compressor Reynolds number of 3.03×10^6 to 0.34×10^6. The measured temperature rise was corrected to

account for heat-transfer effects at the very low inlet pressures. The following changes in compressor performance were noted as the inlet pressure and Reynolds number were decreased:

1. The maximum total-pressure ratio dropped from 1.96 to 1.90.

2. The maximum efficiency point, the maximum flow rate, and the surge point moved progressively to lower flow rates as Reynolds number was lowered.

3. The maximum adiabatic efficiency decreased about 1.5 percentage points as Reynolds number was decreased from near design to 30 percent of the design Reynolds number. From 30 percent to 10 percent of design Reynolds number the maximum efficiency was decreased by about 2.5 percentage points.

4. When the correlating equation

$$\frac{1 - \eta}{1 - \eta_{ref}} = \left[\frac{(Re_U)_{ref}}{Re_U}\right]^n$$

was used, a power of $n = 0.1$ more closely approximated the loss Reynolds number curve for the range of compressor Reynolds number Re_U covered in this investigation than the more commonly used 0.2 power. (η is adiabatic temperature rise efficiency and the subscript ref denotes known reference values.)

5. For a closer approximation of the loss with Reynolds number than is given by a single value of $n = 0.1$, the data can be roughly divided into three parts and the following experimental values of n applied for the corresponding Reynolds number range:

$$n = 0.06, \quad 1.21\times10^6 < Re_U < 3.03\times10^6$$

$$n = 0.09, \quad 0.43\times10^6 < Re_U < 1.21\times10^6$$

$$n = 0.2, \quad 0.34\times10^6 < Re_U < 0.43\times10^6$$

Lewis Research Center,
National Aeronautics and Space Administration,
Cleveland, Ohio, October 29, 1971,
764-74.

APPENDIX A

SYMBOLS

c_p	specific heat at constant pressure of argon, 524 J/(kg)(K); 0.125 Btu/(lbm)(^{o}R)
D	diameter, m; ft
f_{cw}	compressor work factor, $gJc_p(T_6 - T_1)/U_{t3}^2$
g	gravitational acceleration, 9.807 m/sec^2; 32.17 ft/sec^2
ΔH_{is}	isentropic specific work, (N)(m)/kg; (ft)(lbf)/lbm
J	mechanical equivalent of heat, 1.00 (m)(N)/J; 778.16 (ft)(lbf)/Btu
N_s	specific speed, $RPM\sqrt{Q}/60(g\ \Delta H_{is})^{3/4}$
n	exponent
P	total (stagnation) pressure, N/cm^2 abs; psia
p	static pressure, N/cm^2 abs; psia
Q	volume flow, m^3/sec; ft^3/sec
R	gas constant, for argon 208.13 (m)(N)/(kg)(K); 38.683 (ft)(lbf)/(lbm)(^{o}R)
Re_U	compressor Reynolds number, $\rho_1 U_{t3} D_{t3}/\mu_1$
RPM	impeller rotational speed, rpm
T	total (stagnation) temperature, K; ^{o}R
U	impeller wheel speed, m/sec; ft/sec
V	absolute gas velocity, m/sec; ft/sec
w	weight (mass) flow rate, kg/sec; lbm/sec
γ	ratio of specific heat at constant pressure to specific heat at constant volume, for argon 1.667
δ	ratio of compressor inlet total pressure to NASA standard sea-level pressure, $P_1/10.1$ N/cm^2 abs; $P_1/14.7$ psia
η	adiabatic temperature rise efficiency, $T_1\left[(P_6/P_1)^{(\gamma-1)/\gamma} - 1\right]/(T_6 - T_1)$
θ	ratio of compressor inlet total temperature to NASA standard sea-level temperature, $T_1/288.2$ K; $T_1/518.7^{o}$ R
μ	dynamic viscosity, (N)(sec)/m^2; lbm/(sec)(ft)
ρ	total density, kg/m^3; lbm/ft^3

Subscripts:

is	isentropic
m	meridional component
ref	reference values
t	tip
u	tangential component
1	station in inlet pipe upstream of compressor inlet flange (fig. 4)
2	station at impeller inlet
3	station at impeller outlet
4	station at diffuser vane inlet
5	station at diffuser vane outlet
6	station in exit pipe downstream of compressor scroll exit flange (fig. 4)

Superscript:

'	relative to impeller

APPENDIX B

HEAT-TRANSFER EFFECTS ON COMPRESSOR TEMPERATURE RISE

Analysis of the data indicated, particularly at the low Reynolds number, that the measurement of the temperature rise across the compressor was being affected by heat transfer. This was attributed primarily to heat conduction affecting the exit thermocouple readings and, at the lower inlet pressures, heat transfer out of the compressor between the measuring stations.

The six inlet (station 1, fig. 4) thermocouple readings were in good agreement throughout the testing. However, the exit (station 6) thermocouple readings showed a radial temperature difference between the ring of thermocouples near the center of the pipe and those near the pipe wall. The difference in measured compressor temperature rise obtained from the inner and outer thermocouple readings at the exit is shown in figure 10. The temperature rise is shown as a function of inlet pressure for three different flow rates. At the highest inlet pressure (13.7 N/cm^2 abs, or 19.9 psia) the exit thermocouple readings are in close agreement. But, as the inlet pressure and flow were decreased, the temperature rise obtained from the outer ring of thermocouples became progressively lower than that obtained from the inner ring of thermocouples. This difference may be attributed to heat conduction affecting the readings of the outer ring of thermocouples. The potential heat-conduction errors which exist when measuring stream temperatures are discussed in references 3 and 18. So the exit thermocouple readings near the pipe wall (T_{6A}) were not used in computing the compressor temperature rise. The temperature rise calculated by using only the inner ring of exit thermocouples ($T_{6B} - T_1$, fig. 10) shows a gradual decrease in temperature rise, for all but the very low inlet pressures, as the inlet pressure (and thus Reynolds number) decreases. A decrease in temperature rise could be expected to accompany the decrease in inlet pressure due to the increasing boundary layer thickness at the lower Reynolds numbers. The more rapid decrease in temperature rise, computed by using only the inner ring of exit thermocouples, at the very low inlet pressures may have been caused by the combined effects of heat conduction on the thermocouple readings and heat loss from the compressor gas between the measuring stations. When this measured temperature rise, which shows a pronounced decrease at the lower inlet pressures, is used to compute compressor efficiency, the maximum efficiency increases as the Reynolds number decreases at the lower Reynolds numbers. This trend is considered unlikely, since it is opposite to the trend of increasing viscous losses with decreasing Reynolds number and to the fact that the total-pressure-ratio curves progressively decrease.

Heat loss out of the compressor, upstream of the exit measuring station was noted in previous investigations (refs. 4 and 19). One heat path was through the wall behind the

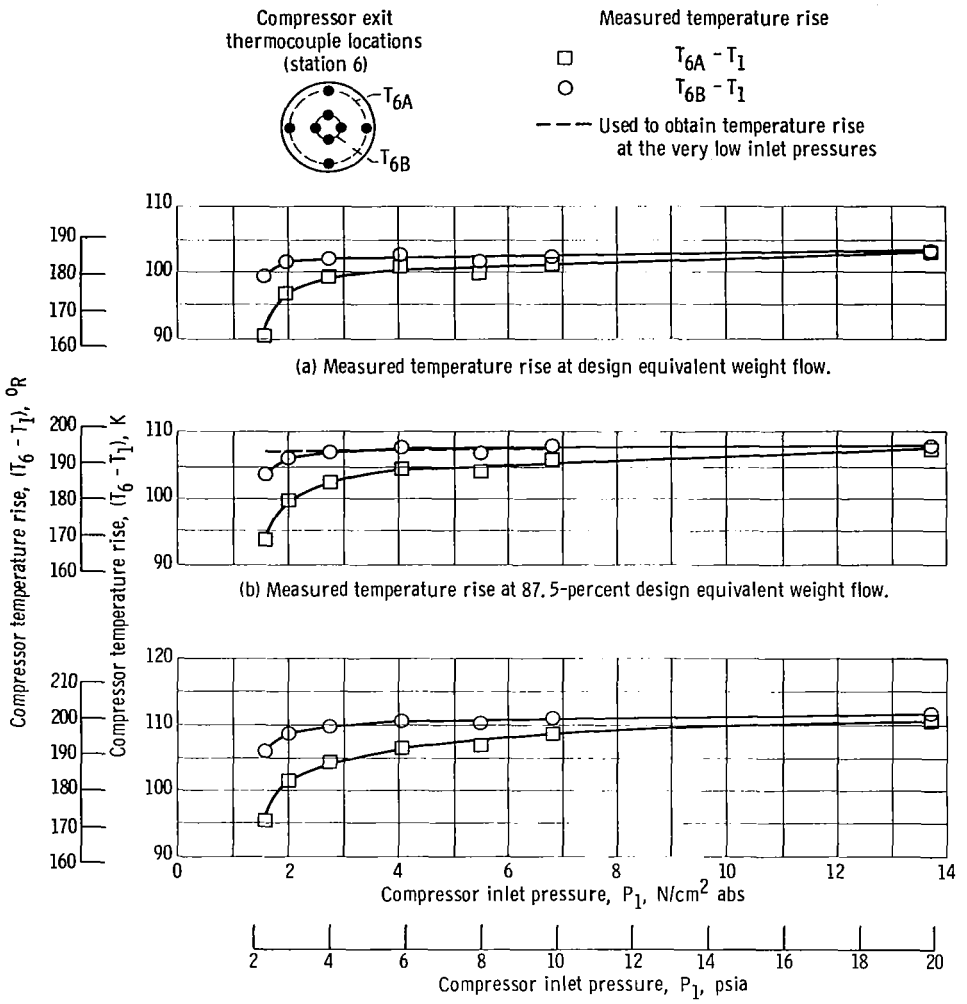

(a) Measured temperature rise at design equivalent weight flow.

(b) Measured temperature rise at 87.5-percent design equivalent weight flow.

(c) Measured temperature rise at 80-percent design equivalent weight flow.

Figure 10. - Comparison of compressor total-temperature rise obtained from inner and outer rings of exit thermocouples as function of inlet pressure, for three flow rates, at 96 percent of design equivalent speed.

rotor to the bearing and seal oil flow. These compressors used a similar bearing and seal arrangement but with oil-jet lubrication rather than the air-oil mist system that was used in this compressor. In the previous investigations an attempt was made to determine the heat loss by measuring the temperature rise of the oil flow due to bearing and seal friction with the compressor evacuated. Then the oil temperature rise due to friction was subtracted from the oil temperature rise measured during performance testing to determine the heat transfer from the compressor gas to the lubricating oil. However, the temperature rise of the air-oil mist was not measured when this test was conducted. It was assumed that the heat transfer with this type of lubrication system would be neg-

ligible. But this heat-transfer path may have been a contributing factor in reducing the exit temperature readings at the lower inlet pressures. As previously mentioned, this low temperature rise gave an unrealistic increase in efficiency at the lower Reynolds numbers. To correct for this, the temperature rise curve ($T_{6B} - T_1$) of figure 10(b) was extrapolated with a straight line (dashed) to obtain values at the lower inlet pressures. The temperature rise curve of figure 10(b) was used because the values were obtained at a flow rate near maximum efficiency. From this curve, a linear decrease in temperature rise from the highest to the lowest inlet pressure was determined to be 1.1 K (2° R). The ratio of the measured total-temperature rise to inlet total temperature based on the temperature measured by the inner ring of thermocouples is shown in figure 11(a). By using the curve of the measured temperature rise ratio obtained at the highest inlet pressure (13.7 N/cm^2 abs, or 19.9 psia), the data points obtained at the lower inlet pressures were proportionally adjusted by using the linear decrease in temperature rise with inlet pressure obtained from figure 10(b). Although the measured temperature rise curves (fig. 11(a)) diverge at the lower flow rates, the three flow rates shown in figure 10

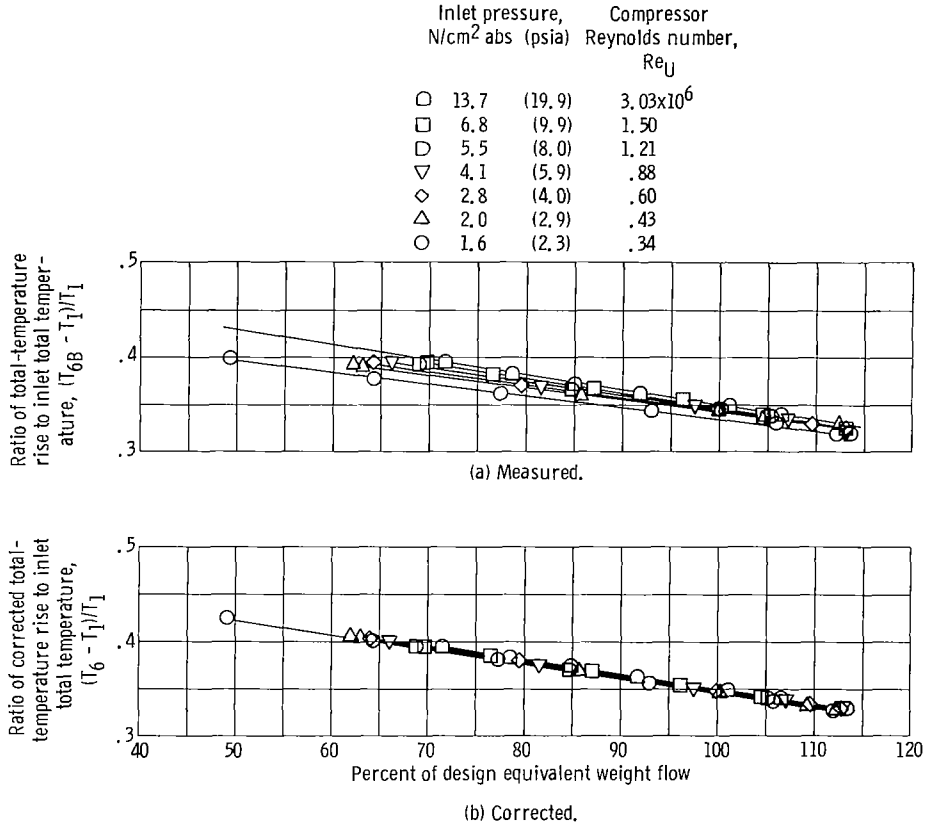

Figure 11. - Ratio of measured and corrected compressor total-temperature rise to inlet total temperature as function of percent of design equivalent weight flow, for seven inlet pressures.

were considered adequate to determine the temperature rise ratio characteristics in the range of maximum efficiency. The corrected total-temperature-rise ratio curves are shown in figure 11(b). The performance data presented in the body of this report were computed by using the corrected curves of figure 11(b).

REFERENCES

1. Glassman, Arthur J.: Summary of Brayton Cycle Analytical Studies for Space-Power System Applications. NASA TN D-2487, 1964.

2. Resnick, B. T.: The Closed Brayton Cycle for Space Power: An Assessment. Paper 66-GT/CLC-10, ASME, Mar. 1966.

3. Perrone, G. L.; and Milligan, H. H.: Brayton Cycle 3.2-Inch Radial Compressor Performance Evaluation. Rep. APS-5214-R, AiResearch Mfg. Co. (NASA CR-54968), May 1966.

4. Heidelberg, Laurence J.; Ball, Calvin L.; and Weigel, Carl: Effect of Reynolds Number on Overall Performance of a 6-Inch Radial Bladed Centrifugal Compressor. NASA TN D-5761, 1970.

5. Heidelberg, Laurence J.; and Ball, Calvin L.: Effect of Reynolds Number on Overall Performance of a 3.7-Inch-Diameter Six-Stage Axial-Flow Compressor. NASA TN D-6628, 1972.

6. Baljé, O. E.: A Study on Reynolds Number Effects in Turbomachines. J. Eng. Power, vol. 86, no. 3, July 1964, pp. 227-235.

7. Bullock, R. O.: Analysis of Reynolds Number and Scale Effects on Performance of Turbomachinery. J. Eng. Power, vol. 86, no. 3, July 1964, pp. 247-256.

8. Stepanoff, Alexey J.: Centrifugal and Axial Flow Pumps. Second ed., John Wiley & Sons, Inc., 1957, pp. 3-6, 72-73.

9. Wong, Robert Y.; Klassen, Hugh A.; Evans, Robert C.; and Winzig, Charles H.: Effect of Operating Parameters on Net Power Output of a 2- to 10-Kilowatt Brayton Rotating Unit. NASA TN D-5815, 1970.

10. Klann, John L.: Steady-State Analysis of a Brayton Cycle Space-Power System. NASA TN D-5673, 1970.

11. Weigel, Carl, Jr.; Tysl, Edward R.; and Ball, Calvin L.: Overall Performance in Argon of 4.25-Inch Sweptback-Bladed Centrifugal Compressor. NASA TM X-2129, 1970.

12. Anon.: Design and Fabrication of the Brayton Cycle High Performance Compressor Research Package. Rep. APS-5269-R, AiResearch Mfg. Co. (NASA CR-72533), Nov. 29, 1967.

13. Ball, Calvin L.; Weigel, Carl, Jr.; and Tysl, Edward R.: Overall Performance of a 6-Inch Radial-Bladed Centrifugal Compressor with Various Diffuser Vane Setting Angles. NASA TM X-2107, 1970.

14. Davis, Hunt; Kottas, Harry; and Moody, A. M. G.: The Influence of Reynolds Number on the Performance of Turbomachinery. Trans. ASME, vol. 73, no. 5, July 1951, pp. 499-509.

15. Shepherd, D. G.: Principles of Turbomachinery. Macmillan Co., 1961, pp. 43-47.

16. Wislicenus, George F.: Fluid Mechanics of Turbomachinery. Vol. 1, Second ed., Dover Publications, Inc., 1965, pp. 54-70.

17. Moody, Lewis F.: Friction Factors for Pipe Flow. Trans. ASME, vol. 66, no. 8, Nov. 1944, pp. 671-684.

18. Futral, Samuel M.; Kofskey, Milton; and Rohlik, Harold E.: Instrumentation Used to Define Performance of Small Size, Low Power Gas Turbines. Paper 69-GT-104, ASME, Mar. 1969.

19. Weigel, Carl; Ball, Calvin L.; and Tysl, Edward R.: Overall Performance in Argon of a 16.4-Centimeter (6.44-Inch) Sweptback-Bladed Centrifugal Compressor. NASA TM X-2269, 1971.

NASA-Langley, 1972 — 1 E-6586